REGULAR ARTICLE

T. Yamamoto · T. Domon · S. Takahashi ·
A. K. S. Arambawatta · M. Wakita

Immunolocalization of proteoglycans and bone-related noncollagenous glycoproteins in developing acellular cementum of rat molars

Abstract To elucidate the roles of proteoglycans (PGs), bone sialoprotein (BSP), and osteopontin (OPN) in cementogenesis, their distribution was investigated in developing and established acellular cementum of rat molars by an immunoperoxidase method. To characterize PGs, antibodies against five species of glycosaminoglycans (GAGs), chondroitin-4-sulfate (C4S), chondroitin-6-sulfate (C6S), unsulfated chondroitin (C0S), dermatan sulfate (DS), and keratan sulfate (KS) were used. Routine histological staining was also applied. With onset of dentin mineralization, the initial cementum appeared on the dentin surface as a hematoxylin-stained fibril-poor layer. Subsequently, primitive principal fibers attached to the initial cementum. As the acellular cementum containing extrinsic fibers covered the initial cementum, the initial cementum formed the cemento-dentinal junction. Following immunohistochemistry at the earliest time of cementogenesis, the initial cementum was intensely immunoreactive for C4S, C6S, C0S, BSP, and OPN. After the initial cementum was embedded, neither the cemento-dentinal junction nor the cementum was immunoreactive for any GAG species. However, the cementum and cemento-dentinal junction were consistently immunoreactive for BSP. Although the cemento-dentinal junction was consistently immunoreactive for OPN, the remaining cementum showed no significant immunoreactivity. Thus, initial acellular cementogenesis requires a dense accumulation of PGs, BSP, and OPN, which may be associated with the mineralization process independently of collagen fibrils and initial principal fiber attachment.

T. Yamamoto (✉) · T. Domon · S. Takahashi ·
A. K. S. Arambawatta · M. Wakita
Department of Oral Health Science, Hokkaido University
Graduate School of Dental Medicine,
Kita13 Nishi7 Kita-Ku,
Sapporo, 060-8586, Japan
e-mail: yamatsu@den.hokudai.ac.jp
Tel.: +81-11-7064225
Fax: +81-11-7064225

Introduction

Cementum is one of dental hard tissues and is composed of mineralized collagen fibers and interfibrillar matrices. It functions as a tooth-supporting device in cooperation with the principal fibers and the alveolar bone proper. The major organic cementum component is composed of collagen fibers, which are classified into two types, the extrinsic (Sharpey's) and intrinsic fibers. The extrinsic fibers are embedded ends of the principal fibers, and the intrinsic fibers are fibers of the cementum proper. On the basis of the distribution of the two kinds of fibers and cells (cementocytes), Schroeder (1986) has established the cementum classification that is now widely used.

Recently, non-collagenous interfibrillar macromolecules have been extensively investigated in the cementum by improved immunohistochemical and biochemical techniques. As a result, many distinct molecules, viz., non-collagenous glycoproteins, proteoglycans (PGs), plasma-derived macromolecules, and other smaller molecules such as growth factors, have been identified (for reviews, see Somerman et al. 1990a; MacNeil and Somerman 1993; Robey 1996; MacNeil et al. 1998; Embery et al. 2000; Waddington and Embery 2001). Bone sialoprotein (BSP) and osteopontin (OPN) belong to the non-collagenous glycoprotein group and are major constituents of the interfibrillar matrices (McKee et al. 1996; Bosshardt et al. 1998; Bosshardt and Nanci 1998; Nanci 1999). BSP and OPN are phosphorylated sialoproteins with Arg-Gly-Asp domains. They are closely associated with mineralization, cell differentiation, matrix–matrix attachment, and cell–cell/matrix attachment in collagen-based hard tissues (for reviews, see Ganss et al. 1999; Sodek et al. 2000).

The PGs are macromolecules composed of core protein and glycosaminoglycans (GAGs). GAGs are linear polysaccharides consisting of repeating disaccharide units and

Table 1 Anti-GAG antibodies and enzymes for pretreatment

Antibody designation	Enzymes used prior to immunostaining	Identified GAG types
2-B-6	Chondroitinase ACII (0.2 U/ml in 0.05 M TRIS–HCl buffer, pH 6.0, at 37°C)	C4S
2-B-6	Chondroitinase B (0.2 U/ml in 0.05 M TRIS–HCl buffer, pH 8.0, at 30°C)	DS
3-B-3	Chondroitinase ABC (0.2 U/ml in 0.05 M TRIS–HCl buffer, pH 8.0, at 37°C)	C0S, C6S
1-B-5	Chondroitinase ABC	C0S
5-D-4	Chondroitinase ABC	KS

are covalently bound to a core protein through a specific sequence of trisaccharides. Several species of GAGs exist: chondroitin sulfate (CS) including chondroitin-4-sulfate (C4S) and chondroitin-6-sulfate (C6S), unsulfated chondroitin (C0S), dermatan sulfate (DS), keratan sulfate (KS), heparan sulfate, heparin, and hyaluronan. Because of their sulfate and carboxyl groups, GAGs are strongly negatively charged and react to basic dyes in histological sections. Individual PGs are classified by the size and amino acid sequence of the core protein and the species of GAGs. Some distinct PGs, viz., small leucine-rich proteoglycans (SLRPs) such as decorin, biglycan, lumican, and fibromodulin, have been suggested to play important roles in the collagen fibril-mineralizing process in cooperation with phosphorylated proteins such as BSP and OPN (for reviews, see Limeback 1991; Goldberg et al. 1995; Linde 1995: Embery et al. 2001).

Immunolocalization of several PG species has been examined in human (Ababneh et al. 1998, 1999), bovine (Bartold et al. 1990; Cheng et al. 1996, 1999), and rat cementum (Matias et al. 2003a). Broadly speaking, lacunae and cementocytes are predominantly immunoreactive sites, and the rest of the cementum including the cemento-dentinal junction shows none or only faint immunoreactivity. In contrast, we have observed human (Yamamoto et al. 1999) and rat cementum (Yamamoto 1986; Yamamoto and Wakita 1990; Yamamoto et al. 2000, 2001) by classical histological and histochemical techniques and have concluded that PGs accumulate at the cemento-dentinal junction. These studies have not determined the species of PGs.

There has been almost no attempt to immunodetect PGs in developing cementum, and thus the way in which PGs are involved in cementogenesis is still unclear. Further, a re-examination of whether PGs accumulate at the cemento-dentinal junction is necessary. To elucidate these questions, the spatial and timed distribution of PGs and related glycoproteins (BSP and OPN) was examined in developing and established acellular cementum (acellular extrinsic fiber cementum) of rat molars by an indirect immunoperoxidase method. To characterize PGs, antibodies against GAGs (C4S, C6S, C0S, DS, and KS) were used.

Materials and methods

This study used ten adult male Wistar rats weighing 250–300 g and 15 3-week-old male Wistar rats weighing about 50 g. The animals and tissue specimens were treated in accordance with the Guidelines of the Experimental Animal Committee, Hokkaido University Graduate School of Dental Medicine.

General histology

After anesthesia by an intraperitoneal injection of sodium pentobarbital, the animals were perfused with 4% paraformaldehyde in 0.1 M phosphate buffer (pH 7.4) for 15 min at room temperature. The upper jaws were dissected out, immersed in the same fixative for 24 h, and demineralized in ethanolic trimethylammonium EDTA (Scott and Kyffin 1978) at 4°C for 2–6 months. Following demineralization, the specimens were dehydrated in a graded series of ethanols and embedded in paraffin. Next, 7-μm-thick serial sections of the first molar were cut mesio-distally and stained with hematoxylin and eosin or silver-impregnated. Some paraffin blocks were used for immunohistochemistry as described below.

Immunohistochemistry

Immunodetection of GAGs

The designation and specificity of primary mouse monoclonal antibodies against GAGs and chondroitinases for pretreatment are detailed in Table 1. All primary antibodies and enzymes were purchased from Seikagaku (Tokyo, Japan). The staining techniques for these antibodies have been established and applied to rat molars (Kaneko et al. 2001), rat salivary glands (Zhao et al. 1998), rabbit alveolar bone (Takagi et al. 1996), and human tooth germs (Zhao et al. 1999).

Deparaffinized sections were immersed in methanol containing 0.3% hydrogen peroxide to inhibit endogeneous peroxidase and pretreated with one of the three chondroitinases. Corresponding chondroitinases were used to generate neoepitopes for the 2-B-6, 3-B-3, and 1-B-5 antibodies and to unmask native epitopes for the 5-D-4 antibody. The sections were incubated successively with the primary antibodies, biotinylated anti-mouse rabbit polyclonal antibody (DAKO Japan, Kyoto, Japan), and streptavidin–biotin–horseradish peroxidase complex (DAKO) and rinsed with phosphate-buffered saline after every incubation. Finally, immunostaining was visualized by the 3,3′-diaminobenzidine method. Normal mouse serum was substituted for the primary antibodies in the negative controls.

Immunodetection of BSP and OPN

For BSP immunodetection, three kinds of antibodies were used as primary antibodies; anti-mouse BSP rabbit polyclonal antibody (LSL, Tokyo, Japan) and anti-human BSP rabbit polyclonal antibodies (Chemicon, Temecula, Canada; Alexis, Lausen, Switzerland). For OPN immunodetection, three kinds of antibodies were used as primary antibodies; anti-mouse OPN rabbit polyclonal antibody (LSL), anti-human OPN mouse monoclonal antibody (American Research Products, Belmont, Mass., USA), and anti-mouse OPN rabbit polyclonal antibody (American Research

Fig. 1 a Overall view of the cervical region of the distal root of the maxillary first molar in adult rats in a hematoxylin and eosin-stained section (*PL* periodontal ligament). Fully developed acellular cementum (*AC* between *arrows*) covers the root dentin (*D*). *Bar* 50 μm. **b** High magnification of the acellular cementum in **a**. The cementodentinal junction (*arrowhead*) is stained most intensely with hematoxylin in the cementum. *Bar* 10 μm. **c** Highly magnified acellular cementum in a silver-impregnated section. The cemento-dentinal junction (*arrowhead*) is observed as an unstained clear layer. The principal fibers (*PF*) form bundles and enter the acellular cementum as extrinsic fibers. *Bar* 10 μm
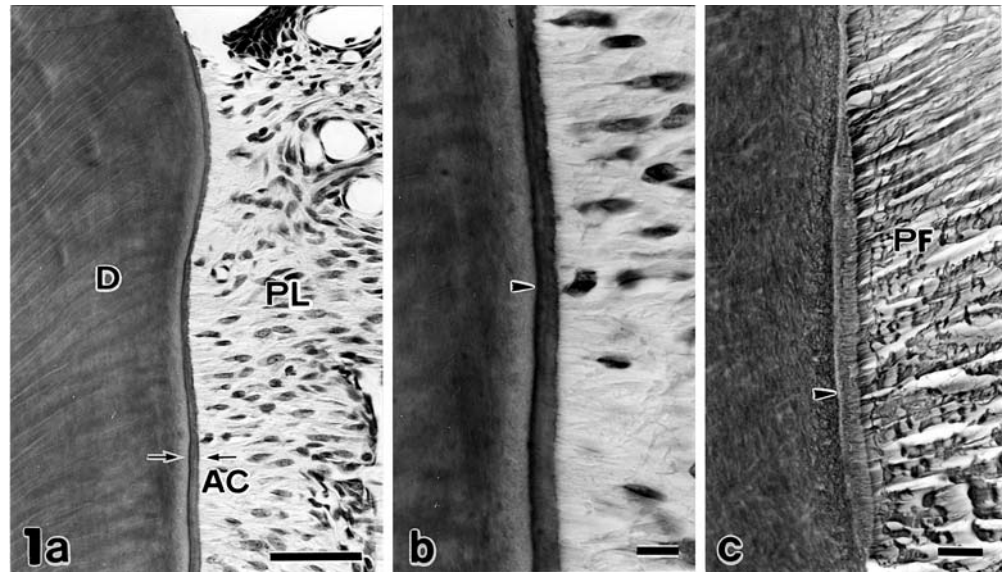
Fig. 2a–e Fully developed acellular cementum (*between arrows*), root dentin (*D*), and principal fibers (*PF*) stained by the 2-B-6 antibody with chondroitinase ACII pretreatment for C4S detection (**a**), the 3-B-3 antibody for C6S and C0S detection (**b**), the 1-B-5 antibody for C0S detection (**c**), the 2-B-6 antibody with chondroitinase B pretreatment for DS detection (**d**), and the 5-D-4 antibody for KS detection (**e**). In all micrographs, the cementum, dentin, and cemento-dentinal junction (*arrowhead*) show no significant immunoreactivity. In some sections, the cementodentinal junction is unclear. The 2-B-6 antibody with chondroitinase ACII (**a**) and chondroitinase B (**d**) pretreatment and the 3-B-3 antibody (**b**) both stain the principal fibers moderately to intensely. The 1-B-5 antibody stains the principal fibers immediately adjacent to the cementum intensely (*small arrowheads*), but the rest of these fibers moderately (**c**). The 5-D-4 antibody stains the principal fibers moderately (**e**). *Bars* 10 μm
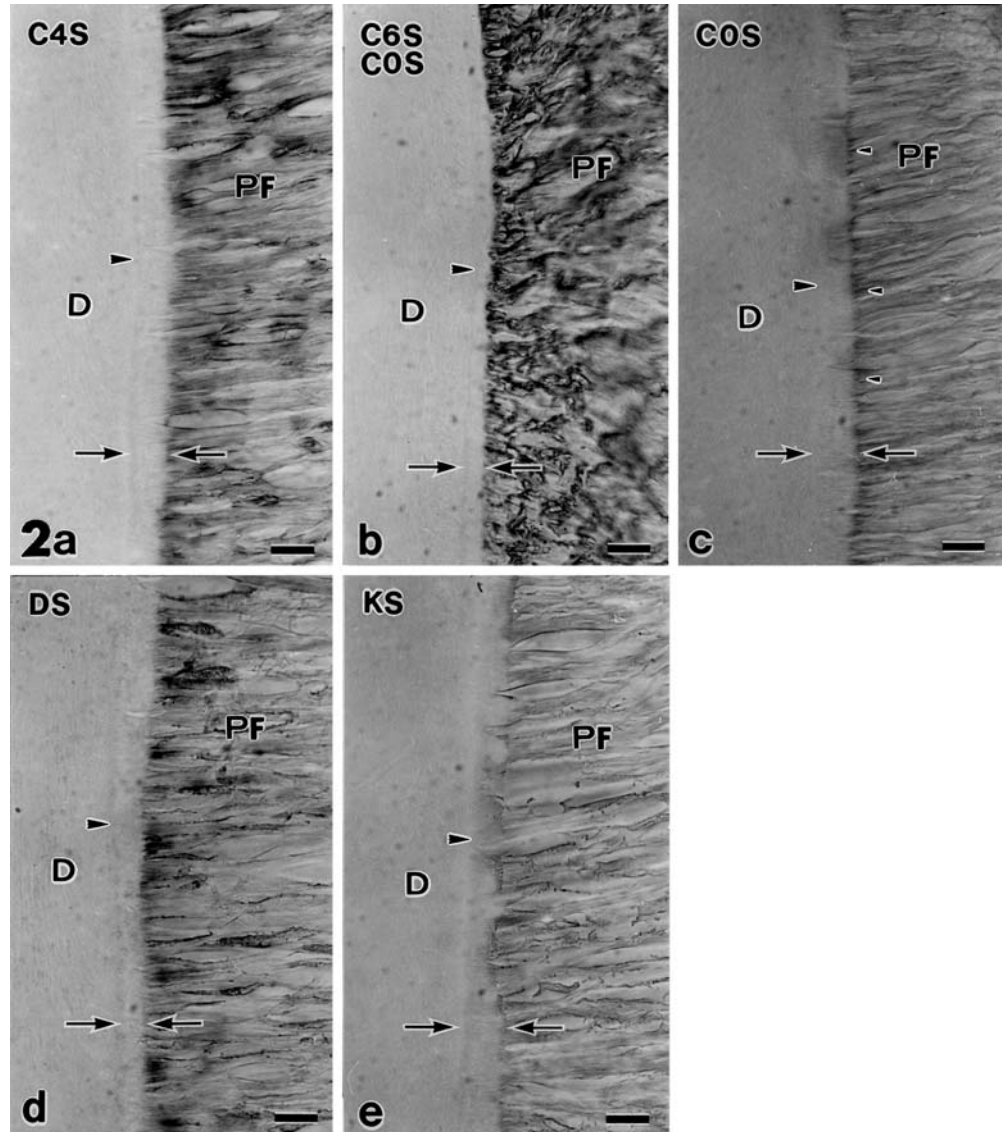
Products). In accordance with the supplier's instructions, these antibodies react to rat antigens in paraffin sections.

After inhibition of endogeneous peroxidase, sections were pretreated with 2.5% testicular hyaluronidase (Sigama, St Louis, Mo., USA). They were then incubated with the primary antibodies, biotinylated anti-mouse rabbit polyclonal antibody or anti-rabbit swine polyclonal antibody (DAKO), and streptavidin–biotin–horse-radish peroxidase complex (DAKO). Immunostaining was visualized as described above. Normal mouse or rabbit serum was substituted for the primary antibodies in the negative controls.

Results

Established acellular cementum

General histology

The distal root of the maxillary first molars was examined in adult rats. The acellular cementum had a thickness of 2–10 μm and stained with hematoxylin. The cemento-dentinal junction took the form of a layer (about 1 μm thick) that was more intensely hematoxylin-stained than the rest of the cementum (Fig. 1a, b). Silver-impregnated sections showed that the cemento-dentinal junction was deficient in collagen fibrils (Fig. 1c). Fully developed principal fibers were arranged at right angles to the cementum surface. The cementum contained the ends of principal fibers as extrinsic fibers.

Immunohistochemistry

GAGs

Neither the cementum nor the cemento-dentinal junction showed immunoreactivity against any of the antibodies (Fig. 2a–e). The 2-B-6 antibody with chondroitinase ACII (Fig. 2a) and chondroitinase B (Fig. 2d) pretreatment and the 3-B-3 antibody (Fig. 2b) stained the principal fibers moderately to intensely. The 1-B-5 antibody intensely stained the principal fibers immediately adjacent to the cementum, but the rest of these fibers were stained moderately (Fig. 2c). The 5-D-4 antibody stained the principal fibers moderately (Fig. 2e).

BSP and OPN

Fundamentally, the three kinds of anti-BSP and anti-OPN antibodies provided a similar labeling pattern for BSP and OPN, respectively. Therefore, sections stained with antibodies purchased from LSL are shown in this study. Tadatomo et al. (2002) have reported the authenticity of these antibodies in a study on root resorption of rat molars.

Anti-BSP antibody stained the cementum moderately and the cemento-dentinal junction intensely (Fig. 3a). Anti-OPN antibody stained the cemento-dentinal junction intensely but did not stain the rest of the cementum

(Fig. 3b). The principal fibers showed moderate to intense immunoreactivity against the two antibodies.
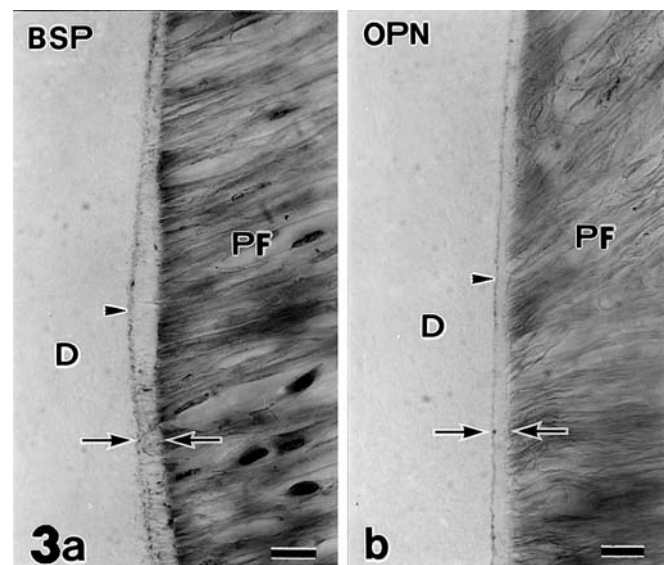
Developing acellular cementum

General histology

The mesial root of the maxillary first molars was examined in 3-week-old rats. For convenience of description, the root was divided into cervical, mid, and apical regions (Fig. 4a).

Apical region At the apical end, Hertwig's epithelial root sheath consisted of two epithelial cell layers. In the cervical direction, dental papilla cells facing the epithelial sheath differentiated into columnar odontoblasts and formed the initial predentin (Fig. 4b). Where the epithelial sheath disintegrated, the epithelial cells became smaller. With the onset of dentin mineralization, hematoxylin-stained initial acellular cementum appeared on the mineralized dentin, and large cementoblasts appeared on the root surface (Fig. 4b). No sign of cellular cemento-genesis was observed.

In silver-impregnated sections (Fig. 5a), collagen fibers in the dental follicle were arranged in parallel with the epithelial sheath at the apical end. More cervically, the fibers were arranged toward the root surface and developed into primitive principal fibers, which attached to the root surface. At this point, a fibril-poor layer appeared between the attached principal fibers and the root surface.

Fig. 3a, b Fully developed acellular cementum (*between arrows*), dentin (*D*), and principal fibers (*PF*) stained with anti-BSP (**a**) and anti-OPN (**b**) antibodies (*arrowhead* cemento-dentinal junction). Anti-BSP antibody stains the cementum moderately and the cemento-dentinal junction intensely. Anti-OPN antibody stains the cemento-dentinal junction intensely but does not stain the bulk of cementum. Both antibodies stain the principal fibers moderately to intensely. *Bars* 10 μm
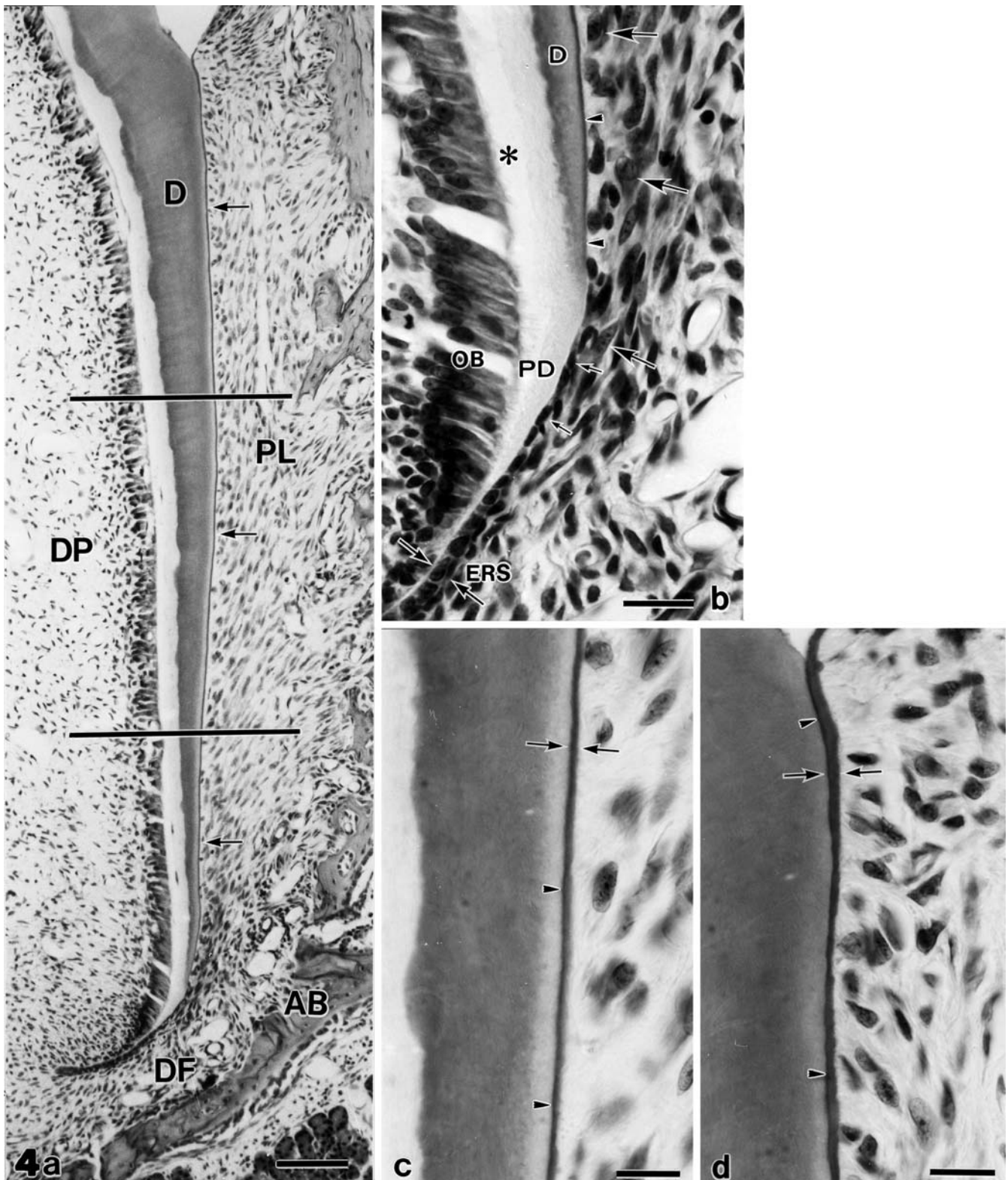
Fig. 4 **a** Overall view of the developing mesial root of the maxillary first molar in 3-week-old rats (*DP* dental pulp, *PL* periodontal ligament, *AB* alveolar bone, *DF* dental follicle); hematoxylin and eosin-stained section. The *two lines* divide the root into apical, mid, and cervical regions, which are magnified in **b**, **c**, and **d**, respectively. Thin acellular cementum (*arrows*) covers the root dentin (*D*). *Bar* 50 μm. **b** The epithelial root sheath (*ERS* between *arrows*) consists of an inner and outer cell layer. More cervically, columnar odontoblasts (*OB*) form predentin (*PD*). The epithelial sheath disintegrates, and the epithelial cells become smaller (*small arrows*). Large cementoblasts (*large arrows*) appear on the root surface. At the onset of dentin mineralization, hematoxylin-stained initial acellular cementum (*arrowheads*) forms on the mineralized dentin (*D*). *Asterisk* Artificial split. *Bar* 20 μm. **c** The intensely hematoxylin-stained cemento-dentinal junction (*arrowheads*) is discernible in the cementum (*between arrows*). *Bar* 20 μm. **d** The acellular cementum (*between arrows*) attains a thickness of 3–5 μm, and the cemento-dentinal junction (*arrowheads*) is more readily discernible than in the mid region. *Bar* 20 μm
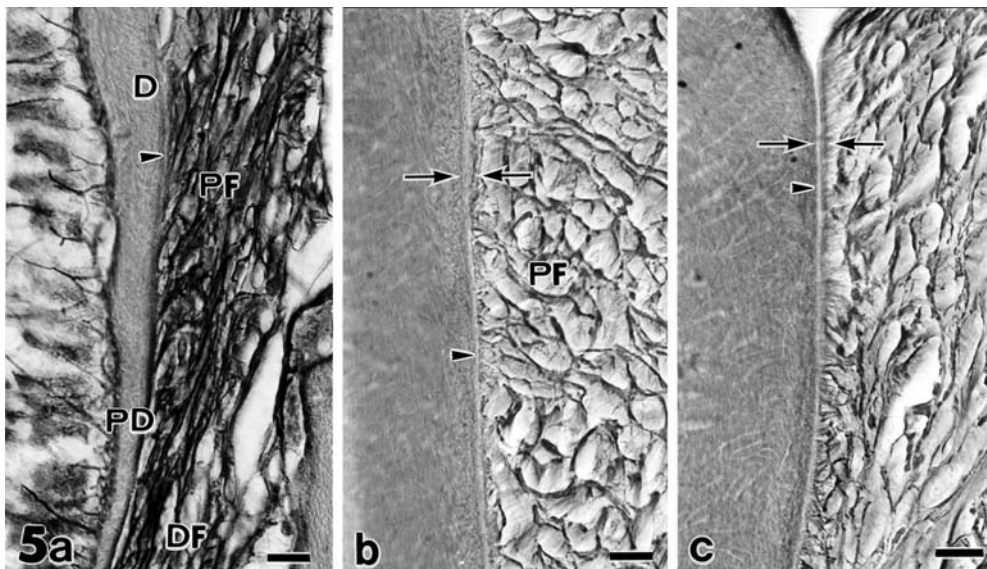
Fig. 5 The apical (**a**), mid (**b**), and cervical (**c**) regions of a silver-impregnated, developing root. **a** The boundary between mineralized dentin (*D*) and predentin (*PD*) is unclear. Collagen fibrils in the dental follicle (*DF*) are arranged in parallel with the predentin. More cervically, the fibrils develop into primitive principal fibers (*PF*). A clear layer that is not silver-impregnated (*arrowhead*) forms between the attached principal fibers and the dentin. *Bar* 10 μm.

b The cementum layer is indicated between *arrows*. The cemento-dentinal junction (*arrowhead*) is discernible as a clear layer. The principal fibers (*PF*) develop into bundles. *Bar* 10 μm. **c** The cementum is indicated *between arrows*. The cemento-dentinal junction (*arrowhead*) is better defined than that in the mid region. *Bar* 10 μm

Mid region The cementum increased in thickness and the principal fibers were well organized. The principal fibers attached on the entire cementum surface. The cemento-dentinal junction, which was intensely stained by hematoxylin and fibril-poor, was discernible in the cementum (Figs. 4c, 5b).

Cervical region The cementum developed to a maximum thickness of 5 μm and the principal fibers were thicker. The cemento-dentinal junction was more obviously discernible than in the mid region (Figs. 4d, 5c).

Immunohistochemistry

GAGs

Apical region At the apical end, after pretreatment with chondroitinase ACII, the 2-B-6 antibody stained odontoblasts and predentin intensely, and the epithelial sheath and dental follicle faintly (Fig. 6a). At the earliest recognizable signs of cementogenesis, the initial cementum and root-related portion of primitive principal fibers showed intense immunoreactivity (Fig. 6b). More cervically, the intense immunoreactivity of principal fibers spread toward the alveolar bone side (Fig. 6a). Predentin lost immunoreactivity abruptly at the mineralization front (Fig. 6b).

At the apical end, the 3-B-3 antibody stained predentin and the dental follicle moderately but did not stain the epithelial sheath or odontoblasts (Fig. 7a). The initial cementum and root-related portion of primitive principal fibers showed intense immunoreactivity (Fig. 7b). More

cervically, the intense immunoreactivity of principal fibers spread toward the alveolar bone side (Fig. 7a). Predentin lost immunoreactivity abruptly at the mineralization front (Fig. 7b).

At the apical end, the 1-B-5 antibody stained predentin intensely but did not stain the epithelial sheath, odontoblasts, or the dental follicle (Fig. 8a). The initial cementum and primitive principal fibers immediately adjacent to the cementum showed intense immunoreactivity (Fig. 8b). The intense immunoreactivity of principal fibers did not spread toward the alveolar bone side (Fig. 8a). Predentin lost immunoreactivity abruptly at the mineralization front (Fig. 8b).

At the apical end, after pretreatment with chondroitinase B, the 2-B-6 antibody stained odontoblasts, the epithelial sheath, predentin, and the dental follicle moderately to intensely (Fig. 9a). The initial cementum showed no immunoreactivity. Developing principal fibers were moderately immunoreactive. They did not show specific one-sided staining (Fig. 9b). Predentin lost immunoreactivity abruptly at the mineralization front (Fig. 9b).

Mid and cervical region None of the anti-GAG antibodies stained the cementum or the cemento-dentinal junction. The 2-B-6 antibody (Fig. 6c, d, following chondroitinase ACII pretreatment; Fig. 9c, d, following chondroitinase B pretreatment) and the 3-B-3 antibody (Fig. 7c, d) stained the principal fibers moderately to intensely. The 1-B-5 antibody stained the principal fibers immediately adjacent to the cementum moderately to intensely but stained the rest of these fibers more weakly (Fig. 8c, d).

The immunostaining pattern with the 5-D-4 antibody (not shown) was similar to that obtained by the 2-B-6

antibody with chondroitinase B pretreatment through the apical to cervical regions.

BSP and OPN

Sections stained with antibodies purchased from LSL are shown.

Apical region At the apical end, both the anti-BSP and anti-OPN antibodies stained odontoblasts, predentin, and the dental follicle moderately to intensely. Predentin lost immunoreactivity abruptly at the mineralization front (Figs. 10a, 11a). In the epithelial sheath, anti-BSP antibody intensely stained the epithelial cells and inner basal membrane facing the odontoblasts. Anti-OPN antibody intensely stained the inner basal membrane but the epithelial cells only weakly. Both antibodies stained the initial cementum very intensely. Anti-BSP antibody stained developing principal fibers moderately, and anti-OPN antibody stained them moderately to intensely (Figs. 10a, 11a).

Mid and cervical region Anti-BSP antibody stained the cementum moderately to intensely, and the principal fibers moderately (Fig. 10b, c). The anti-OPN antibody stained the cemento-dentinal junction and the principal fibers moderately to intensely but did not stain the rest of cementum (Fig. 11b, c). In this experiment, the control sections showed no positive reaction.

Discussion

Previous histological and histochemical studies have found that the initial cementum or the cemento-dentinal junction of rat molars is a fibril-poor layer (1–2 μm thick), which is stained intensely with hematoxylin, reacts positively to periodic acid/Sciff, alcian blue, and ruthenium red, and is markedly methachromatic to toluidine blue (Paynter and Pudy 1958; Owens 1980; Yamamoto 1986; Yamamoto and Wakita 1990; Yamamoto et al. 2000, 2001). This indicates that the initial cementum contains strongly negatively charged polysaccharides. Developmentally, the fibril-poor superficial root dentin (about 1 μm thick) remains unmineralized for a short period of time after the onset of the initial dentin mineralization (Owens 1980; Yamamoto and Wakita 1990). Ruthenium-red-positive matrices then appear in this layer and fill the space, undergoing mineralization. Developing principal fibers are then attached to and embedded in the matrices (Yamamoto and Wakita 1990). From these findings, we have suggested: (1) the negatively charged polysaccharides are GAGs of PGs and, during the earliest part of acellular cementogenesis, some PGs are deposited in the unmineralized superficial dentin and act as an adhesive for the initial principal fiber attachment; (2) the deposition of PGs prior to the fiber attachment results in the fibril-poor PG-rich cemento-dentinal junction; (3) the PGs remain at

the cemento-dentinal junction in the established cementum and act as an adhesive for the dentin and cementum.

In general, PGs are easily lost during histological processing, especially during demineralization. Here, we have used ethanolic trimethylammonium EDTA for demineralization to preserve the PGs and glycoproteins without reducing the antigenicity (Scott and Kyffin 1978; Takagi et al. 1992, 1996). None of the anti-GAG antibodies used in this study stains the established acellular cementum or the cemento-dentinal junction. Previous immunohistochemical studies have detected neither PGs nor GAGs at the cemento-dentinal junction in human teeth (Ababneh et al. 1998, 1999), bovine teeth (Bartold et al. 1990; Cheng et al. 1996, 1999), or rat molars (Matias et al. 2003a). The cemento-dentinal junction, however, is immunoreactive for BSP and OPN. Therefore, the main macromolecules containing negatively charged polysaccharides are probably not PGs but acid glycoproteins, viz., OPN and BSP, although there is also the possibility that a small amount of PGs and/or transformed PGs are present at undetectable levels. Functional details of the two glycoproteins will be discussed later.

Neither the established acellular cementum nor the cemento-dentinal junction contained significant amounts of PGs. Developmentally, however, the initial cementum and root-related principal fibers were intensely immunoreactive for C4S and C0S at the earliest onset of cementogenesis. This cementogenesis site also showed intense immunoreactivity against the 3-B-3 antibody, which recognizes both C6S and C0S. C6S is probably also localized here, because the 3-B-3 antibody reacts to C6S more strongly than to C0S (Couchmann et al. 1984). In addition, the initial cementum was intensely immunoreactive for BSP and OPN. These findings suggest that C4S-containing, C0S-containing, and C6S-containing PGs, and BSP and OPN are closely associated with initial acellular cementogenesis.

Some species of SLRPs, especially CS-decorin and CS-biglycan are essential for biological mineralization (Limeback 1991; Goldberg et al. 1995; Linde 1995; Embery et al. 2001). BSP and OPN are also very important for mineralization as mineralization-initiating and mineralization-inhibiting factors, respectively (Bosky 1995; Ganss et al. 1999; Sodek et al. 2000; Goldberg et al. 2001). Therefore, a major part of the accumulated PGs appears to be decorin and biglycan and to be closely involved in the mineralization of the initial cementum in cooperation with BSP and OPN.

The roles of PGs in mineralization have been investigated in detail in the collagen fibril-mineralizing process (Limeback 1991; Linde 1995: Goldberg et al. 1995; Embery et al. 2001). Here, CS-decorin and CS-biglycan regulate collagen fibril assembly to make it suitable for future mineralization. Decorin (probably C4S-decorin) occupies the gap zones between collagen molecules. The CS chains bind calcium ions and retain them in the gap zones. Proteoglycanases or matrix metalloproteinases degrade the PGs so that the CS chains
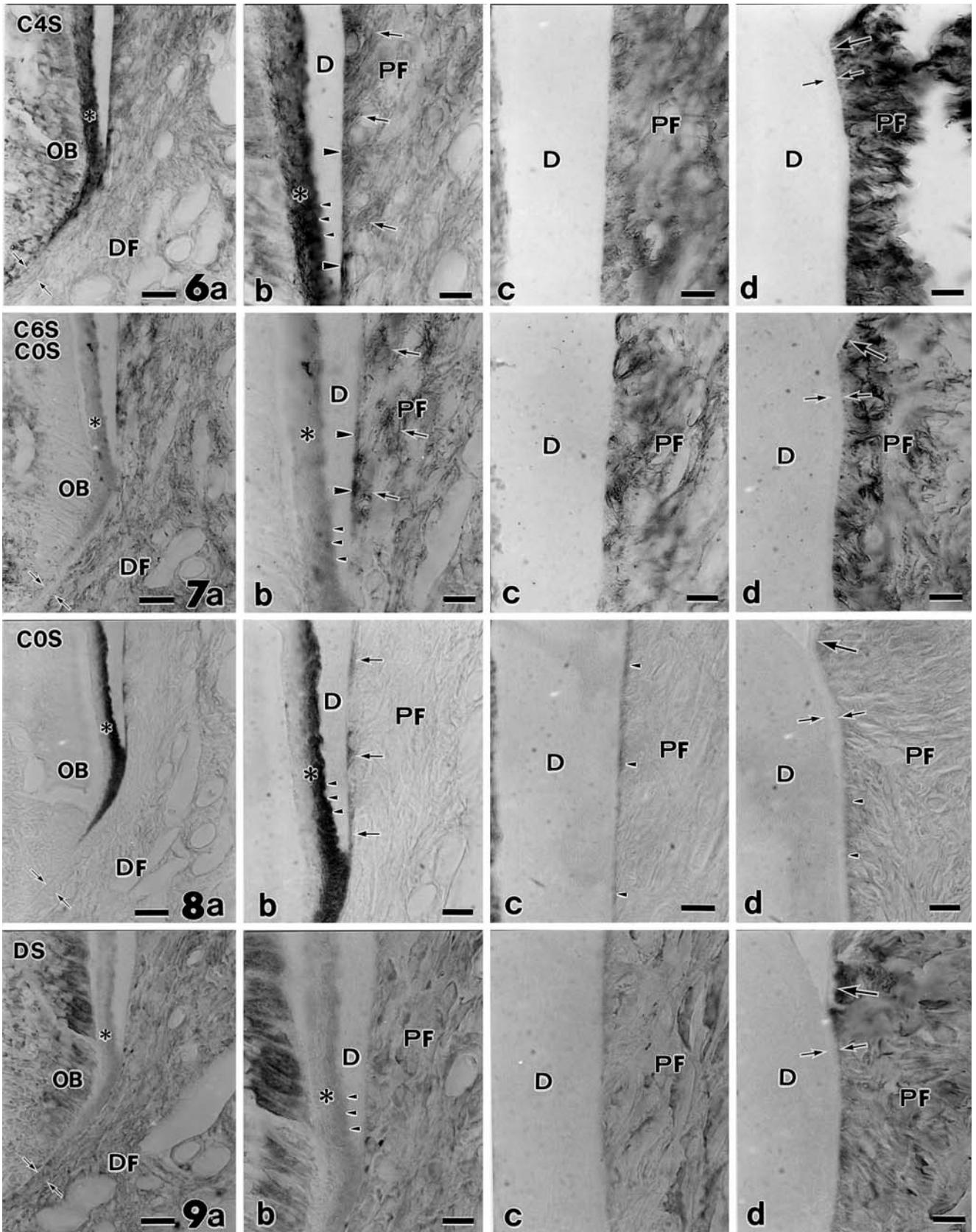
◀ **Fig. 6a–d** Developing root stained by the 2-B-6 antibody with chondroitinase ACII pretreatment for C4S detection. The apical (**a**, **b**), mid (**c**), and cervical regions (**d**) are shown (*OB* odontoblasts, *DF* dental follicle, *D* dentin, *PF* principal fibers, *asterisks* predentin). **a** The antibody stains odontoblasts and predentin intensely, and the epithelial root sheath (*between arrows*) and dental follicle faintly. **b** The antibody stains the initial cementum (*large arrowheads*) and root-related portion (*arrows*) of principal fibers intensely. Traced cervically, the intense staining of principal fibers spreads toward the alveolar bone side (see **a**). The staining of predentin disappears abruptly at the mineralization front (*small arrowheads*). **c** The antibody stains the principal fibers intensely but does not stain the cementum or cemento-dentinal junction. **d** The antibody stains the principal fibers intensely but does not stain the cementum or the cemento-dentinal junction. The cementum (*between arrows*) can be identified only at the most cervical area. The *large arrow* indicates detached and/or enamel-covering cementum. *Bars* 20 μm (**a**), 10 μm (**b–d**)

Fig. 7a–d Developing root stained with the 3-B-3 antibody for C6S and C0S detection. The apical (**a**, **b**), mid (**c**), and cervical (**d**) regions are shown (*OB* odontoblasts, *DF* dental follicle, *D* dentin, *PF* principal fibers, *asterisks* predentin). **a** The antibody stains predentin and dental follicle moderately but does not stain the epithelial sheath (*between arrows*) or odontoblasts. **b** The antibody stains the initial cementum (*large arrowheads*) and root-related portion (*arrows*) of principal fibers intensely. Traced cervically, the intense staining of the principal fibers spreads toward the alveolar bone side (see **a**). The staining of predentin disappears abruptly at the mineralization front (*small arrowheads*). **c** The antibody stains the principal fibers intensely but does not stain the cementum or cemento-dentinal junction. **d** The antibody stains the principal fibers intensely but does not stain the cementum or cemento-dentinal junction. The cementum (*between arrows*) can be identified only at the most cervical area. The *large arrow* indicates detached and/or enamel-covering cementum. *Bars* 20 μm (**a**), 10 μm (**b–d**)
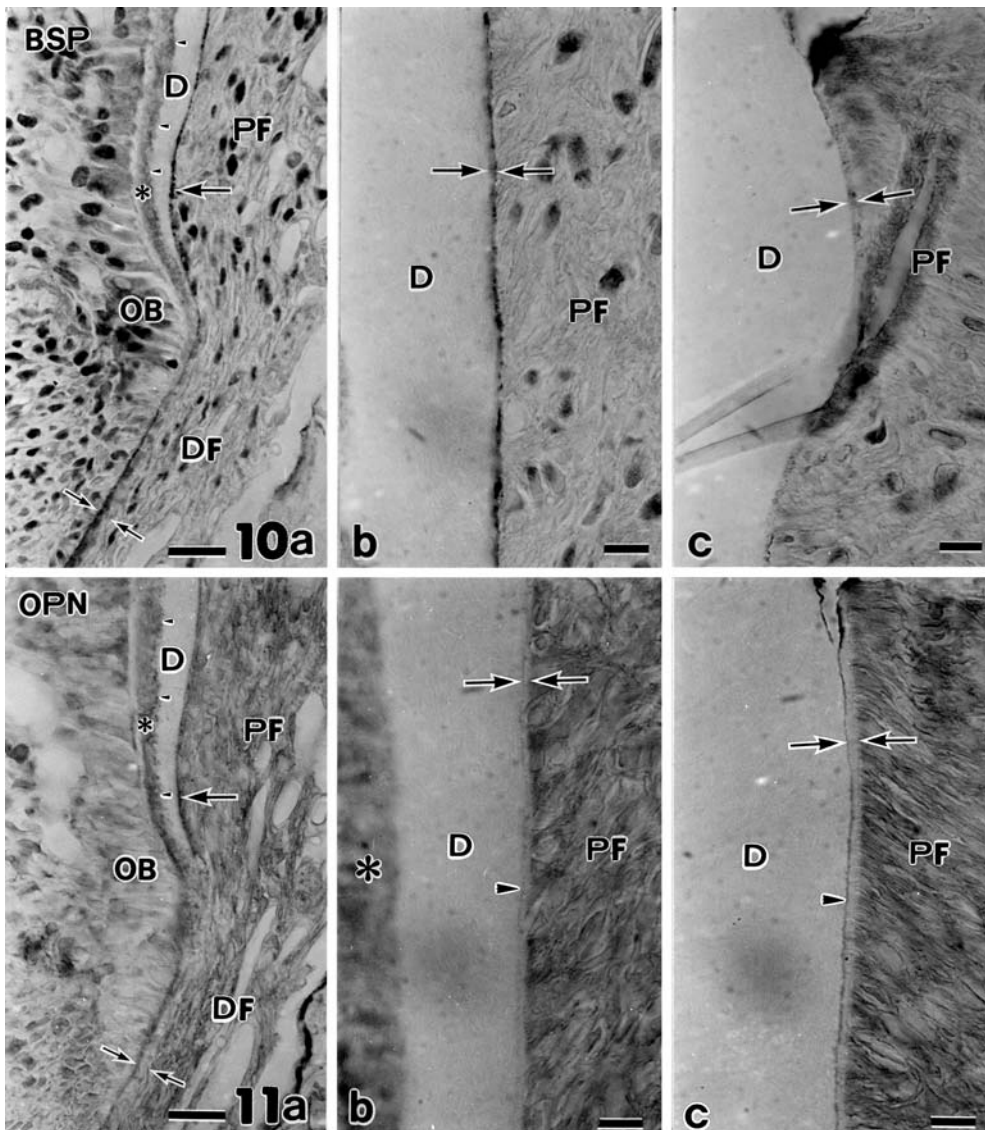
Fig. 8a–d Developing root stained with the 1-B-5 antibody for C0S detection. The apical (**a**, **b**), mid (**c**), and cervical (**d**) regions are shown (*OB* odontoblasts, DF dental follicle, *D* dentin, *PF* principal fibers, *asterisks* predentin). **a** The antibody stains predentin intensely but does not stain the epithelial sheath (*between arrows*), odontoblasts, or dental follicle. **b** The antibody stains the initial cementum and principal fibers immediately adjacent to the cementum intensely (*arrows*). The intense staining of principal fibers does not spread toward the alveolar bone side (see **a**). The staining of predentin disappears abruptly at the mineralization front (*arrowheads*). **c, d** The antibody stains the principal fibers immediately adjacent to the cementum moderately to intensely (*arrowheads*) but the rest of these fibers more weakly. The cementum or cemento-dentinal junction is not stained. The cementum (**d**, *between arrows*) can be identified only at the most cervical area. The *large arrow* in **d** indicates detached and/or enamel-covering cementum. *Bars* 20 μm (**a**), 10 μm (**b–d**)

Fig. 9a–d Developing root stained by the 2-B-6 antibody with chondroitinase B pretreatment for DS detection. The apical (**a**, **b**), mid (**c**), and cervical (**d**) regions are shown (*OB* odontoblasts, DF dental follicle, *D* dentin, *PF* principal fibers, *asterisks* predentin). **a** The antibody stains odontoblasts, the epithelial sheath (*between arrows*), predentin, and dental follicle moderately to intensely. **b** The antibody does not stain the initial cementum. The principal fibers were moderately stained throughout the periodontal ligament. The staining of predentin disappears abruptly at the mineralization front (*arrowheads*). **c** The antibody stains the principal fibers moderately but does not stain the cementum or cemento-dentinal junction. **d** The antibody stains the principal fibers moderately to intensely. The cementum or cemento-dentinal junction is not stained. The cementum (*between arrows*) can be identified only at the most cervical area. The *large arrow* indicates detached and/or enamel-covering cementum. *Bars* 20 μm (**a**), 10 μm (**b–d**)

are detached from the core protein, and calcium ions are released to future mineralization sites. The core protein remains in the gap zones and binds phosphoproteins such as BSP (bone and cementum) and phosphophoryn (dentin). Immobilized phosphates then bind calcium ions in the gap zones and act as mineralization nucleators. Localized increases in phosphate ions by alkaline phosphatase activity encourage the precipitation of additional calcium–phosphate complexes in the gap zones. These precipitates rapidly convert to the first hydroxyapatite crystals. Eventually, hydroxyapatite crystals spread between collagen fibers to mineralize the tissue fully. During this process OPN may act as an inhibitory regulator against hydroxyapatite overgrowth (Bosky 1995; Sodek et al. 2000; Goldberg et al. 2001).

The proposed model applies to the sites at which there are pre-existing collagen fibrils. The initial cementum, however, is deficient in collagen fibrils. Under such conditions, successive mineralization spreading from the mineralized dentin may not occur. Yamamoto (1986) has observed isolated calciferous spherules on the initial acellular cementum before principal fiber attachment. Following principal fiber attachment, no calciferous spherules can be observed, and cementum mineralization advances along the principal fibers; Yamamoto (1986) has suggested that the calciferous spherules are derived from matrix vesicles. Iwamatsu (1993) has found that alkaline phosphatase is most active in the periodontal ligament at the earliest acellular cementogenesis of mouse molars. On the basis of these data, we propose that the initial acellular cementum is mineralized in a fashion independent of collagen fibrils, i.e., the calciferous spherules, which are added anew from the periodontal ligament side, induce the entire mineralization of the initial cementum. During this mineralization process, BSP and OPN act as mineralization-initiating and mineralization-inhibiting factors, respectively, and PGs act as calcium-capture points in addition to facilitating principal fiber assembly. A highly dense accumulation of PGs, BSP, and OPN is required for this process, probably because of the lack of stable mineralization media (collagen fibrils). This view is supported by Bosshardt and Nanci (2003), who have suggested that a dense accumulation of the two glycoproteins induces mineralization of collagen-free cementicle-like structures. After principal fiber attachment, mineralization may advance in the proposed fashion dependent on collagen fibrils.

Once PGs have been involved in mineralization, they may be almost completely degraded so that no GAG species are detectable in the cementum or at the cemento-dentinal junction. In bovine cementum, decorin and biglycan carry C4S, but no C6S (Cheng et al. 1999). In dentin mineralization, as described above, C4S-decorin is a major calcium ion capture-point. C6S-PGs may not be as effective as C4S-PG for initial cementogenesis. The initial cementum is immunoreactive for C0S. Takagi et al. (1990) have immunodetected C0S in rat incisor predentin, but the direct contribution of C0S-PGs to biomineralization is still

Fig. 10a–c Developing root stained with anti-BSP antibodies. The apical (**a**), mid (**b**), and cervical (**c**) regions are shown (*OB* odontoblasts, *DF* dental follicle, *D* dentin, *PF* principal fibers, *asterisks* predentin). **a** The antibody stains the initial cementum (*arrow*) very intensely, and odontoblasts, predentin, and dental follicle moderately to intensely. Developing principal fibers are moderately stained. In the epithelial root sheath (*between arrows*), epithelial cells and the inner basal membrane facing differentiating odontoblasts are intensely stained. Predentin loses staining abruptly at the mineralization front (*arrowheads*). **b** The antibody stains the cementum (*between arrows*) intensely and the principal fibers moderately. **c** The antibody stains the cementum (*between arrows*) moderately to intensely, and principal fibers moderately. *Bars* 20 µm (**a**), 10 µm (**b, c**)

Fig. 11a–c Developing root stained with anti-OPN. The apical (**a**), mid (**b**), and cervical (**c**) regions are shown (*OB* odontoblasts, *DF* dental follicle, *D* dentin, *PF* principal fibers, *asterisks* predentin). **a** The antibody stains the initial cementum (*arrow*) very intensely, and the epithelial sheath (*between arrows*), predentin, odontoblasts, dental follicle, and developing principal fibers moderately to intensely. In the epithelial sheath, the intense staining is confined to the inner basal membrane facing differentiating odontoblasts. Predentin loses the staining abruptly at the mineralization front (*arrowheads*). **b** The antibody stains the principal fibers and the cemento-dentinal junction (*arrowhead*) moderately to intensely but does not stain the rest of cementum (*between arrows*). **c** The antibody stains the principal fibers moderately to intensely. The cemento-dentinal junction (*arrowhead*) showed more intense immunoreactivity than in the mid region. The cementum (*between arrows*) lacks staining. *Bars* 20 µm (**a**), 10 µm (**b, c**)

unclear. C0S might be produced during the degradation of C4S-PGs and/or C6S-PGs (Byers et al. 1997).

During biomineralization, BSP and OPN play multifunctional roles other than as a mineralization initiator (BSP) and inhibitor (OPN; for reviews, see Ganss et al. 1999; Sodek et al. 2000). In cementogenesis, the two glycoproteins have been proposed as being involved in the

differentiation and attachment of cementoblasts (Somerman et al. 1990b; MacNeil et al. 1994, 1995a, 1996) and in the integration of cementum (McKee et al. 1996; Bosshardt et al. 1998; Nanci 1999). To date, the factors inducing cementoblast differentiation have still not been finally established.

In this context and considering the matrix-binding affinity of BSP and OPN, we propose that, at initial cementogenesis, the two glycoproteins bind primitive principal fibers at the root surface. After the cementum is fully formed, the two glycoproteins maintain the structural integrity of the cementum and act as a binding material for the dentin and cementum. The last point is supported by the evidence that OPN and BSP accumulate at the bone–bone interface or cement line (McKee et al. 1993; Chen et al. 1994; McKee and Nanci 1996a, 1996b; Nanci 1999). However, it may be too hasty a conclusion to assume that these glycoproteins are the most important for cemento-dentinal attachment. Indeed, OPN knock-out mice do not show major changes in bone structure (Rittling et al. 1998), and this raises questions about whether glycoproteins such as BSP and OPN are primarily essential in mineralized tissue cohesion (Nanci 1999). In addition, when mineral formation and its deposition are inhibited in non-specific alkaline phosphatase knock-out mice, the deposition of the non-collagenous matrix is also prevented, and as a result, the principal fibers are not firmly anchored by Sharpey's fibers (Beertsen et al. 1999). The solidity of the cemento-dentinal junction may be based on a complex system of glycoprotein adhesion, mineral deposition, fibril interdigitation, and other factors.

Our findings concerning BSP and OPN immunolocalization are inconsistent with previous light-microscopic findings by other authors. The inconsistencies can be summarized into three points. (1) In this study, cementum matrices other than the cemento-dentinal junction do not stain for OPN. Sasano et al. (2001) and Tadatomo et al. (2002) have also shown that the cemento-dentinal junction is the only immunoreactive site for OPN in rat acellular cementum. However, it is generally accepted that the acellular cementum stains for OPN other than at the cemento-dentinal junction. Indeed, Bronckers et al. (1994), who have examined undemineralized sections of rat molars, have shown intense immunoreactivity for OPN in the entire acellular cementum. (2) In our study, the anti-BSP and anti-OPN antibodies stain predentin intensely but do not stain dentin. Similar findings have been obtained in rat incisors (Ohma et al. 2002) and molars (Sasano et al. 2001; Hosoya et al. 2003). Tadatomo et al. (2002) and Matias et al. (2003b) have also presented micrographs in which dentin is almost completely immuno-negative for BSP in rat molars. However, because BSP and OPN are generally considered to exist mainly in mineralized matrices, dentin would have been more intensely stained than predentin. Indeed, dentin stains much more intensely for OPN than predentin in the micrographs of undemineralized sections published by Bronckers et al. (1994). Other studies have demonstrated no obvious differences in the immunoreactivity of dentin and predentin; both kinds of tissue are only faintly stained in mouse molars (OPN: Somerman et al. 1990b; BSP: MacNeil et al. 1994), in mouse incisors (BSP and OPN: MacNeil et al. 1995a), rat molars (BSP: Lekic et al. 1996a), and in porcine teeth (BSP and OPN: Chen et al. 1993), or, as in porcine teeth (Suzuki et al. 2002), neither of them shows immunoreac-

tivity for OPN. (3) This study has immunodetected BSP and OPN throughout the periodontal ligament. Sasano et al. (2001), Tadatomo et al. (2002), and Hosoya et al. (2003) have also presented micrographs in which the periodontal ligament is immunoreactive for BSP and OPN in rat molars. However, BSP, unlike OPN, is generally considered to be highly specific to mineralized tissues. Other studies have immunodetected BSP only along the root surface in mouse incisors (MacNeil et al. 1995a), mouse molars (MacNeil et al. 1994, 1995a, 1995b), and dog premolars (Matsuura et al. 1995) or have immunodetected no BSP in the periodontal ligament in rat molars (Lekic et al. 1996a, 1996b; Matias et al. 2003b) or human teeth (Ivanovski et al. 2001).

Following an examination of previous light-microscopic studies, we have found that studies supporting our findings involve the use of buffered-paraformaldehyde for fixation and EDTA for demineralization (Sasano et al. 2001; Ohma et al. 2002; Tadatomo et al. 2002; Hosoya et al. 2003), whereas most other studies employ other chemicals: 95% ethanol (Somerman et al. 1990b), Bouin's fixative (MacNeil et al. 1994, 1995b), and 10% formalin (Ivanovski et al. 2001) for fixation; acetic acid (MacNeil et al. 1994, 1995b) and 0.2N HCl (Chen et al. 1993; Lekic et al. 1996a, 1996b) for demineralization. Buffered-paraformaldehyde and EDTA are generally recommended for the immunohistochemistry of mineralized tissue, because different chemicals often cause unstable and misleading immunoreactions. In particular, strong acid often damages antigenicity during demineralization. In accordance with Väänänen and Korhonen (1984), EDTA is the only demineralization medium used in immunohistochemistry for which valid information is available. For this reason, we suggest that the inconsistencies between our and previous studies arise mainly from the differences in tissue-processing (not from the different antibody species), and that our findings are more standard for demineralized rat molars at the light-microscopic level.

Regarding point (1) mentioned above, for the determination of the exact OPN immunoreactive site, the acellular cementum should be fixed and demineralized adequately, sectioned in a suitable direction, and magnified sufficiently in micrographs. Our micrographs and sections, like those of Sasano et al. (2001) and Tadatomo et al. (2002), satisfy these conditions. Regarding point (2), Sasano et al. (2001) have also found that predentin is intensely immunoreactive for BSP and OPN, whereas dentin shows little immunoreactivity. With regard to the low immunoreactivity of dentin, they suggest that epitopes for the antibodies are masked in mineralized dentin, or that some epitopes are lost with calcium during demineralization. We agree with this assessment; indeed, similar effects may also be taken into consideration for point (1), the almost complete immuno-negativity for OPN in the bulk of mineralized cementum. Our immunohistochemical data imply that odontoblasts synthesize BSP and OPN actively. In situ hybridization cannot however detect transcripts for BSP mRNA, unlike those for OPN mRNA, in odontoblasts during root dentinogenesis in rat (Sasano et al.

2001) or mouse molars (MacNeil et al. 1995a, 1996). We have not found a satisfactory answer to this question. Regarding point (3), our finding is not quite unexpected, because the principal fibers may absorb serum BSP from the blood stream (Ganss et al. 1999; Nanci 1999; Sodek et al. 2000). By electron microscopy, however, neither BSP nor OPN has been immunodetected in the periodontal ligament of adequately processed rat molars and human teeth (McKee et al. 1996; Bosshardt et al. 1998). An answer to this inconsistency awaits further investigation.

It is still uncertain whether the initial cementum layer is of epithelial or cementoblastic origin. The epithelial sheath cells show no immunoreactivity for C0S or C6S and only faint immunoreactivity for C4S. With respect to BSP and OPN, cementoblasts have been confirmed to secrete these two glycoproteins as cementum constituents by in situ hybridization and immunohistochemistry (Chen et al. 1992, 1993; Bronckers et al. 1994; MacNeil et al. 1996, 1998; Sommer et al. 1996; Sasano et al. 2001; Suzuki et al. 2002). Although, in our study, the epithelial sheath is immunoreactive for the two proteins, the epithelial cells appear to decrease in number and cell activity prior to the onset of cementogenesis. Kaneko et al. (1999) have reported that epithelial sheath cells migrate into the periodontal ligament or die immediately after the onset of root dentin formation in rat molars. In contrast, cementoblasts have been shown to be highly secretory cells with well-developed intracellular organelles, rough endoplasmic reticulum, Golgi apparatus, and secretory granules. Many cementoblasts extend cellular processes containing secretory granules to the root surface (Yamamoto 1986; Cho and Garant 1988, 1989, 2000; Diekwisch 2001). Diekwisch (2001) has argued that there are no epithelial products on the root dentin surface. From these findings, we suggest that the cementoblasts secrete PGs, BSP, and OPN as cementum constituents, despite this study having failed to demonstrate specific intracellular immunolabeling of cementoblasts for these molecules. The function of the BSP and OPN of the epithelial sheath is unclear, although Somerman et al. (1990b) have suggested that the epithelial sheath secretes OPN, which induces the attachment and differentiation of cementoblasts.

Cementoblast progenitors have generally been considered to be dental follicle cells. Recently some studies have proposed that epithelial sheath cells undergo transformation into cementoblasts, and secrete cementum matrices such as BSP and OPN (Thomas 1995; Bosshardt and Nanci 1997, 1998; Bosshardt et al. 1998). However, there is no general agreement on this yet (Cho and Garant 2000; Diekwisch 2001).

Many studies have detected GAGs and PGs in the periodontal ligament of human (Larjava et al. 1992; Häkkinen et al. 1993; Ababneh et al. 1998, 1999), bovine (Watanabe and Kubota 1998; Cheng et al. 1999), rat (Fujii and Hirabayashi 1999; Kaneko et al. 2001; Sato et al. 2002; Matias et al. 2003a), and mouse teeth (Häkkinen et al. 2000). Although there are minor species-dependent differences, CS and DS are common GAGs, and decorin and biglycan (CS-SLRPs) are common PGs. Other PGs include versican (high molecular weight CS-PG), lumican and fibromodulin (KS-SLRPs), heparan sulfate-PGs, and hyaluronan. It is well known that the SLRPs modulate collagen fibrillogenesis and enhance collagen fibril stability (for a review, see Iozzo 1998). The PGs in the rat periodontal ligament may belong mainly to the SLRPs, and the SLRPs may regulate principal fiber structure during cementogenesis (Matias et al. 2003a) and in response to various environmental conditions (Häkkinen et al. 2000; Kaneko et al. 2001).

References

Ababneh KT, Hall RC, Embery G (1998) Immunolocalization of glycosaminoglycans in aging, healthy and periodontally diseased human cementum. Arch Oral Biol 43:235–246

Ababneh KT, Hall RC, Embery G (1999) The proteoglycans of human cementum: immunohistochemical localization in healthy, periodontally involved and aging teeth. J Periodontal Res 34:87–96

Bartold PM, Reinboth B, Nakae H, Narayanan AS (1990) Proteoglycans of bovine cementum. Matrix 10:10–19

Beertsen W, VandenBos T, Everts V (1999) Root development in mice lacking functional tissue non-specific alkaline phosphatase gene: inhibition of acellular cementum formation. J Dent Res 78:1221–1229

Bosky AL (1995) Osteopontin and related phosphorylated sialoproteins: effects on mineralization. Ann N Y Acad Sci 760:249–256

Bosshardt DD, Nanci A (1997) Immunodetection of enamel- and cementum-related (bone) proteins at the enamel-free area and cervical portion of tooth in rat molars. J Bone Miner Res 12:367–379

Bosshardt DD, Nanci A (1998) Immunolocalization of epithelial and mesenchymal matrix constituents in association with inner enamel epithelial cells. J Histochem Cytochem 46:135–142

Bosshardt DD, Nanci A (2003) Immunocytochemical characterization of ectopic enamel deposits and cementicles in human teeth. Eur J Oral Sci 111:51–59

Bosshardt DD, Zalzal S, McKee MD, Nanci A (1998) Developmental appearance and distribution of bone sialoprotein and osteopontin in human and rat cementum. Anat Rec 250:13–33

Bronckers ALJJ, Farach-Carson MC, Waveren E van, Butler WT (1994) Immunolocalization of osteopontin, osteocalcin, and dentin sialoprotein during dental root formation and early cementogenesis in the rat. J Bone Miner Res 9:833–841

Byers S, Rooden JC van, Foster BK (1997) Structural changes in the large proteoglycan, aggrecan, in different zones of the ovine growth plate. Calcif Tissue Int 60:71–78

Couchmann JR, Caterson B, Christner JE, Baker JR (1984) Mapping by monoclonal antibody detection of glycosaminoglycans in connective tissues. Nature 307:650–652

Chen J, Shapiro HS, Sodek J (1992) Development expression of bone sialoprotein mRNA in rat mineralized connective tissue. J Bone Miner Res 7:987–997

Chen J, McCulloch CA, Sodek J (1993) Bone sialoprotein in developing porcine dental tissues: cellular expression and comparison of tissue localization with osteopontin and osteonectin. Arch Oral Biol 38:241–249

Chen J, McKee MD, Nanci A, Sodek J (1994) Bone sialoprotein mRNA expression and ultrastructural localization in fetal porcine calvarial bone: comparison with osteopontin. Histochem J 26:67–78

Cheng H, Caterson B, Neame PJ, Lester GE, Yamauchi M (1996) Differential distribution of lumican and fibromodulin in tooth cementum. Connect Tissue Res 34:87–96

Cheng H, Caterson B, Yamauchi M (1999) Identification and immunolocalization of chondroitin sulfate proteoglycans in tooth cementum. Connect Tissue Res 40:37–47

Cho MI, Garant PR (1988) Ultrastructural evidence of directed cell migration during initial cementoblast differentiation in root formation. J Periodontal Res 23:268–276

Cho MI, Garant PR (1989) Radioautographic study of (^{3}H) mannose utilization during cementoblast differentiation, formation of acellular cementum, and development of periodontal ligament principal fibers. Anat Rec 223:209–222

Cho MI, Garant PR (2000) Development and general structure of the periodontium. Periodontology 24:9–27

Diekwisch TSH (2001) The developmental biology of cementum. Int J Dev Biol 45:695–706

Embery G, Waddington RJ, Hall RC, Last KS (2000) Connective tissue elements as diagnostic aids in periodontology. Periodontology 24:193–214

Embery G, Hall R, Waddington R, Septier D, Goldberg M (2001) Proteoglycans in dentinogenesis. Crit Rev Oral Biol Med 12:331–349

Fujii T, Hirabayashi Y (1999) Histochemical studies of glycosaminoglycans in developing periodontal ligaments of ICR mouse. Anat Rec 254:465–473

Ganss B, Kim RH, Sodek J (1999) Bone sialoprotein. Crit Rev Oral Biol Med 10:79–98

Goldberg M, Septier D, Lécole S, Chardin H, Quintana MA, Acevedo AC, Gafni G, Dillouya D, Vermelin L, Thonemann B, Scmalz G, Bissila-Mapahou P, Carreau JP (1995) Dental mineralization. Int J Dev Biol 39:93–110

Goldberg HA, Warner KJ, Li MC, Hunter GK (2001) Binding of bone sialoprotein, osteopontin and synthetic polypeptides to hydroxyapatite. Connect Tissue Res 42:25–37

Häkkinen L, Oksala O, Salo T, Rahemtulla F, Larjava H (1993) Immunohistochemical localization of proteoglycans in human periodontium. J Histochem Cytochem 41:1689–1699

Häkkinen L, Strassburger S, Kähäri V-M, Scott PG, Eichstetter I, Iozzo RV, Larjava H (2000) A role for decorin in the structural organization of periodontal ligament. Lab Invest 80:1869–1880

Hosoya A, Yoshiba K, Yoshiba N, Hoshi K, Iwaku M, Ozawa H (2003) An immunohistochemical study on hard tissue formation in a subcutaneously transplanted rat molar. Histochem Cell Biol 119:27–35

Iozzo RV (1998) Matrix proteoglycans: from molecular design to cellular function. Annu Rev Biochem 67:609–652

Ivanovski S, Li H, Haase HR, Bartold PM (2001) Expression of bone associated macromolecules by gingival and periodontal ligament fibroblasts. J Periodontal Res 36:131–141

Iwamatsu Y (1993) Histochemical and electron microscopical study during the development of the mouse molar periodontal ligament (in Japanese). Jpn J Conserv Dent 36:252–270

Kaneko H, Hashimoto S, Enokiya Y, Ogiuchi H, Shimono M (1999) Cell proliferation and death of Hertwig's epithelial root sheath in the rat. Cell Tissue Res 298:95–103

Kaneko S, Ohashi K, Soma K, Yanagishita M (2001) Occlusal hypofunction causes changes of proteoglycan content in the rat periodontal ligament. J Periodontal Res 36:9–17

Larjava H, Häkkinen L, Rahemtulla F (1992) A biochemical analysis of human periodontal tissue proteoglycans. Biochem J 284:267–274

Lekic P, Sodek J, McCulloch CA (1996a) Osteopontin and bone sialoprotein expression in regenerating rat periodontal ligament and alveolar bone. Anat Rec 244:50–58

Lekic P, Sodek J, McCulloch CA (1996b) Relationship of cellular proliferation to expression of osteopontin and bone sialoprotein in regenerating rat periodontium. Cell Tissue Res 285:491–500

Limeback H (1991) Molecular mechanisms in dental hard tissue mineralization. Curr Opin Dent 1:826–835

Linde A (1995) Dentin mineralization and the role of odontoblasts in calcium transport. Connect Tissue Res 33:163–170

MacNeil RL, Somerman MJ (1993) Molecular factors regulating development and regeneration of cementum. J Periodontal Res 28:550–559

MacNeil RL, Sheng N, Strayhorn C, Fisher LW, Somerman MJ (1994) Bone sialoprotein is located to the root surface during cementogenesis. J Bone Miner Res 9:1597–1606

MacNeil RL, Berry J, D'Errico J, Strayhorn C, Piotroski B, Somerman MJ (1995a) Role of two mineral-associated adhesion molecules, osteopontin and bone sialoprotein, during cementogenesis. Connect Tissue Res 33:323–329

MacNeil RL, Berry J, D'Errico J, Strayhorn C, Somerman MJ (1995b) Localization and expression of osteopontin in mineralized and non mineralized tissues of periodontium. Ann N Y Acad Sci 760:166–176

MacNeil RL, Berry J, Strayhorn C, Somerman MJ (1996) Expression of bone sialoprotein mRNA by cells lining the mouse tooth root during cementogenesis. Arch Oral Biol 41:827–835

MacNeil RL, D'Errioco JA, Ouyang H, Berry J, Strayhorn C, Somerman MJ (1998) Isolation of murine cementoblasts: unique cells or uniquely-positioned osteoblasts? Eur J Oral Sci 106:350–356

Matias MA, Li H, Young WG, Bartold PM (2003a) Immunohistochemical localization of fibromodulin in the periodontium during cementogenesis and root formation in the rat molar. J Periodontal Res 38:502–507

Matias MA, Li H, Young WG, Bartold PM (2003b) Immunohistochemical localization of extracellular matrix proteins in the periodontium during cementogenesis in the rat molar. Arch Oral Biol 48:709–716

Matsuura M, Herr Y, Han KY, Lin WL, Genco RJ, Cho MI (1995) Immunohistochemical expression of extracellular matrix components of normal and healing periodontal tissues in the beagle dog. J Periodontol 66:905–914

McKee MD, Nanci A (1996a) Osteopontin: an interfacial extracellular matrix protein in mineralized tissues. Connect Tissue Res 35:195–205

McKee MD, Nanci A (1996b) Osteopontin at mineralized tissue interface in bone, teeth, and osseointegrated implants: ultrastructural distribution and implications for mineralized tissue formation, turn over, and repair. Microsc Res Tech 33:141–164

McKee MD, Farach-Carson MC, Butler WT, Hauschka DV, Nanci A (1993) Ultrastructural immunolocalization of non collagenous (osteopontin and osteocalcin) and plasma (albumin and α_2HS-glycoprotein) proteins in rat bone. J Bone Miner Res 8:485–496

McKee MD, Zalzal S, Nanci A (1996) Extracellular matrix in tooth cementum and mantle dentin: localization of osteopontin and other noncollagenous proteins, plasma proteins, and glycoconjugates by electron microscopy. Anat Rec 245:293–312

Nanci A (1999) Content and distribution of noncollagenous matrix proteins in bone and cementum: relationship to speed of formation and collagen packing density. J Struct Biol 126:256–269

Ohma N, Takagi Y, Takano Y (2002) Distribution of noncollagenous dentin matrix proteins and proteoglycans, and their relation to calcium accumulation in bisphosphonate-affected rat incisors. Eur J Oral Sci 108:222–232

Owens PDA (1980) A light and electron microscopic study of the early stages of root surface formation in molar teeth in the rat. Arch Oral Biol 24:901–907

Paynter KJ, Pudy G (1958) A study of the structure, chemical nature, and development of cementum in the rat. Anat Rec 131:233–251

Rittling SR, Matsumoto HN, McKee MD, Nanci A, An X, Novick KE, Kowalski AJ, Noda M, Denhardt DT (1998) Mice lacking osteopontin show normal development and bone structure but display altered osteoclast formation in vitro. J Bone Miner Res 13:1101–1111

Robey PG (1996) Vertebrate mineralized matrix proteins: structure and function. Connect Tissue Res 35:131–136

Sasano Y, Maruya Y, Sato H, Zhu J-X, Takahashi I, Mizoguchi I, Kagayama M (2001) Distinctive expression of extracellular matrix molecules at mRNA and protein levels during formation of cellular and acellular cementum in the rat. Histochem J 33:91–99

Sato R, Yamamoto H, Kasai K, Yamauchi M (2002) Distribution of versican, linkprotein and hyaluronic acid in the rat periodontal ligament during experimental tooth movement. J Periodontal Res 37:15–22

Schroeder HE (1986) Cementum. In: Schroeder HE (ed) The periodontium. Springer, Berlin Heidelberg New York, pp 23–127

Scott JE, Kyffin TW (1978) Demineralization in organic solvents by alkylammonium salts of ethylenediaminetetra-acetic acid. Biochem J 169:697–701

Sodek J, Ganss B, McKee MD (2000) Osteopontin. Crit Rev Oral Biol Med 11:279–303

Somerman MJ, Morrison GM, Alexander MB, Foster RA (1990a) Structure and composition of cementum. In: Bowen W, Tadak L (eds) Cariology of the 1990s. University of Rochester, New York, pp 155–171

Somerman MJ, Shroff B, Agraves WS, Morrison G, Craig AM, Denhard DT, Foster RA, Sauk JJ (1990b) Expression of attachment proteins during cementogenesis. J Biol Buccale 18:207–214

Sommer B, Bickel M, Hofstetter W, Wetterwald A (1996) Expression of matrix proteins during the development of mineralized tissues. Bone 19:371–380

Suzuki M, Inoue T, Shimono M, Yamada S (2002) Behavior of epithelial root sheath during tooth root formation in porcine molars: TUNEL, TEM, and immunohistochemical studies. Anat Embryol 206:13–20

Tadatomo Y, Komatsu M, Kagayama M (2002) Immunohistochemical studies on physiological root resorption of rat molars (in Japanese). Jpn J Oral Biol 44:282–292

Takagi M, Hishikawa H, Hosokawa Y, Kagami A, Rahemtulla F (1990) Immunohistochemical localization of glycosaminoglycans and proteoglycans in predentin and dentin of rat incisors. J Histochem Cytochem 38:319–324

Takagi M, Maeno M, Kagami A, Takahashi Y, Otsuka K (1992) Biochemical and lectin- and immunohistochemical studies of solubility and retention of bone matrix proteins during EDTA demineralization. Histochem J 24:78–85

Takagi M, Maeno M, Yamada T, Miyashita K, Otsuka K (1996) Nature and distribution of chondroitin sulfate and dermatan sulfate proteoglycans in rabbit alveolar bone. Histochem J 28:341–351

Thomas HF (1995) Root formation. Int J Dev Biol 39:231–237

Väänänen HK, Korhonen LK (1984) Immunohistochemical techniques for calcified tissues. In: Dickson GR (ed) Methods of calcified tissue preparation. Elsevier, Amsterdam, pp 309–332

Waddington RJ, Embery G (2001) Proteoglycans and orthodontic movement. J Orthod 28:281–290

Watanabe T, Kubota T (1998) Characterization of fibromodulin isolated from bovine periodontal ligament. J Periodontal Res 33:1–7

Yamamoto T (1986) The innermost layer of cementum: its ultrastructure, development, and calcification. Arch Histol Jpn 49:459–481

Yamamoto T, Wakita M (1990) Initial attachment of principal fibers to the root dentin surface in rat molars. J Periodontal Res 25:113–119

Yamamoto T, Domon T, Takahashi S, Islam N, Suzuki R, Wakita M (1999) The structure and function of the cemento-dentinal junction in human teeth. J Periodontal Res 34:261–268

Yamamoto T, Domon T, Takahashi S, Islam MN, Suzuki R, Wakita M (2000) The structure of the cemento-dentinal junction in rat molars. Ann Anat 182:185–190

Yamamoto T, Domon T, Takahashi S, Islam MN, Suzuki R (2001) The initial attachment of cemental fibrils to the root dentin surface in acellular and cellular cementogenesis in rat molars. Ann Anat 183:123–128

Zhao M, Takata T, Ogawa I, Miyauchi M, Ito H (1998) Localization of glycosaminoglycans (GAGs) in pleomorphic adenoma (PA) of salivary glands: an immunohistochemical evaluation. J Oral Pathol Med 27:272–277

Zhao M, Lu Y, Takata T, Ogawa I, Miyauchi M, Mock D, Nikai H (1999) Immunohistochemical and histochemical characterization of the mucosubstances of odontogenic mixoma: histogenesis and differential diagnosis. Pathol Res Pract 195:391–397